

# CHAPTER 1

## HYDRIDE VAPOR PHASE EPITAXY OF GROUP III NITRIDE MATERIALS

Vladimir Dmitriev and Alexander Usikov\*  
*Technologies and Devices International, Inc.,*  
*12214 Plum Orchard Dr., Silver Spring, MD 20904, USA*  
\**e-mail: usikov@tdii.com*

In this chapter we describe recent experimental results on hydride vapor phase epitaxy (HVPE) of group III nitride materials including epitaxial layers and multi-layer device structures. Properties of GaN, InN, AlN, and AlGaIn layers grown by HVPE are presented. For GaN layers, n-type and p-type doping during HVPE growth is reported. Thick crack free AlN layers grown by stress control HVPE are described. New directions in HVPE technology including large area growth, multi-wafer growth, sub-micron multi-layer growth, and fabrication of nano-size structures including GaN and InN nanowires are briefly discussed. Properties of HVPE grown AlGaIn/GaN hetero structures with two-dimensional electron and two dimensional hole gases are presented. Applications of HVPE grown group III nitride materials including substrate applications (template substrates, free standing substrates, and bulk substrates) and device structures for both optoelectronic application (blue and ultraviolet light emitting diodes grown by HVPE) and electronic applications (high electron mobility transistors grown by HVPE) are discussed as well.

### 1. Introduction

The HVPE technology has been demonstrated to deposit single crystal layers of both GaN<sup>1</sup> and AlN<sup>2</sup> more than 30 years ago. Fig. 1 illustrates the basic idea of the method. For GaN growth, source materials are

gallium chloride and ammonia gases. Gallium chloride is formed inside growth apparatus by a reaction of gaseous HCl and Ga metal. Formed gallium chloride is transported into a growth zone of the apparatus where it reacts with ammonia forming GaN. Substrates are located in the growth zone and, if growth conditions including substrate parameters are suitable, single crystal GaN is formed on the substrate. The method provides deposition rates of several microns per minute making it possible to grow hundred microns thick layers.

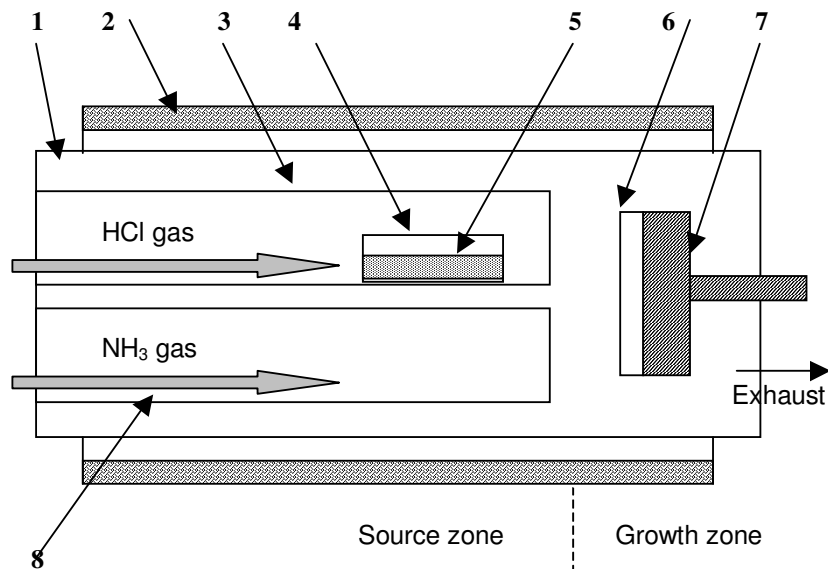


Fig. 1. Schematic illustration for GaN HVPE growth: 1 - main reactor tube, 2 - heating elements, 3 - Ga source gas channel, 4 - boat with Ga melt, 5 - Ga melt, 6 - substrate, 7 - substrate holder, and 8 - ammonia source tube.

Due to well recognized potential of GaN materials for light emitters, numerous attempts to create GaN-based blue light emitting diodes by HVPE, including the demonstration of the first GaN violet light emitter,<sup>3</sup> have been taken in the 70<sup>th</sup>. AlGaIn alloy growth by HVPE has also been performed.<sup>4</sup> However, despite substantial progress in material quality and process understanding, background n-type carrier concentration in grown

materials remained high and p-type GaN materials have not been fabricated by that time.

Rapid progress in another epitaxial technology, metal organic chemical vapor deposition (MOCVD) for p-type GaN and AlGaIn materials in the early 90<sup>th</sup>,<sup>5,6</sup> and its ability to form Ga(Al)N/InGaIn quantum well structures made this method a technology of choice for the fabrication of GaN-based devices including green, blue, ultra violet (UV), and eventually white light emitting diodes (LEDs).<sup>7</sup> The MOCVD was also the first epitaxial method to make GaN-based laser diodes (LDs) and high performance electronic devices. However, many material issues in the field remain unsolved. Due to absence of native GaN and AlN substrates, GaN-based LEDs and HEMTs are currently manufacturing by MOCVD and molecular beam epitaxy (MBE) on foreign substrates, sapphire or silicon carbide. A poor lattice match and difference of thermal expansion coefficient for these substrates usually lead to the formation of threading defects in the epitaxial layers, cracking of layers during the post growth cooling, and residual strains in the epitaxial layers. These defects contribute to high background doping and degrade both electrical and optical properties of the layers and devices.

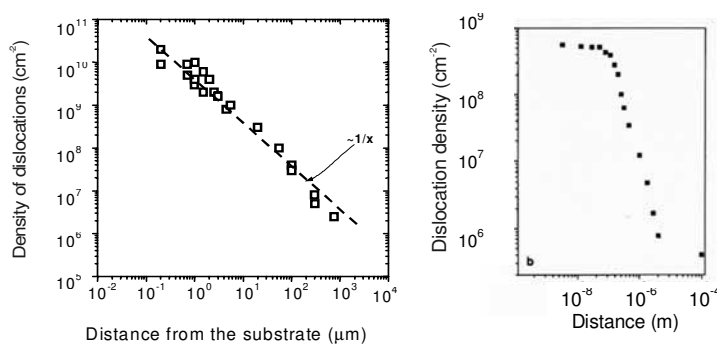


Fig. 2. Defect density in GaN layers vs. layer thickness. Left picture: GaN grown by HVPE on sapphire<sup>12</sup>. Right picture: GaN layers grown by HVPE on 6H-SiC substrate<sup>13</sup>.

In the 90<sup>th</sup>, focus of HVPE development for GaN materials shifted to substrate applications<sup>8,9</sup>. Slow progress and substantial technical obstacles in other crystal growth techniques to form bulk GaN or AlN crystals, put HVPE method on a leading position to produce substrate

materials for group III nitride semiconductor devices. High deposition rate intrinsic to GaN HVPE method and ability to form thick single crystal GaN layers on foreign substrates have led to intense developments in the field and to the demonstration of the first large area (3 cm diameter) GaN free standing wafers.<sup>10</sup> The later developments of HVPE technology for free standing GaN wafers resulted in GaN materials with a record room temperature electron mobility of 1320 cm<sup>2</sup>/V sec and donor concentration of 7.8x10<sup>15</sup>cm<sup>-3</sup>.<sup>11</sup> It was demonstrated by several research teams that dislocation density in GaN HVPE layers decreases dramatically with layer thickness increase (Fig. 2).<sup>12</sup>

For thick GaN layers grown on SiC substrates, dislocation density measured by transmission electron microscopy (TEM) was about 1x10<sup>7</sup> and 4x10<sup>5</sup>cm<sup>-2</sup> at 10 and 100 microns distance from SiC/GaN interface, respectively.<sup>13</sup> Growth of thick GaN layers and subsequent fabrication of low defect free standing GaN wafers led to the fabrication of advanced GaN-based power devices' high-frequency transistors, and blue lasers. Currently, HVPE technology is established for commercial production of various types of GaN and AlN substrate materials (Section 5). For more than 30 years of GaN HVPE development various designs of growth apparatuses and process arrangements were described in numerous scientific publications.<sup>14,15,16</sup> In this paper we report on our recent results on the fabrication and characterization of GaN, AlN, InN, AlGaIn, and InGaIn materials and heterostructures by HVPE. We also describe several novel directions in HVPE technology for group III nitrides such as multi-layer sub micron device structures, nano-structures, and large area HVPE growth.

## 2. Experiment

Group III nitride materials described in this paper were grown on proprietary homebuilt HVPE growth equipment. The growth processes were carried out in atmospheric pressure on a multi-wafer HVPE machines having a hot wall quartz tube reactors with a resistively heated multi zone furnaces (Fig. 3). Ammonia (NH<sub>3</sub>) and hydrogen chloride (HCl) were used as active gases and argon served as a carrier gas. Ga, Al,

and In metals were used as group III source materials. The metals were located in boats placed in separate channels in the source zone of the growth machine. Substrates were placed on a holder, which got in and out from the growth zone of the reactor by a quartz moving rod. Usually we use sapphire or silicon carbide substrates. Substrate capacity of the growth machines was up to seven 2-inch wafers. Size of the substrates ranged from 2 to 6-inch.

Typical growth temperature varied from 900 to 1100°C, except for InN grown at lower temperatures (Section 3.7). For n-type doping, silane ( $\text{SiH}_4$ ) gas was used. To grow p-type layers, Mg and/or Zn metals were placed in the source zone of the reactor. Growth rate was controlled from 0.05 to 1 microns per min by changing HCl flow through the corresponding metal source channel. Thickness of grown layers was varied from a few nanometres to several millimetres and was controlled by the growth rate and deposition time. The machine design allows us to grow multi layer hetero structures with thick ( $>10 \mu\text{m}$ ) and thin ( $<0.1 \mu\text{m}$ ) layers in the same epitaxial process.

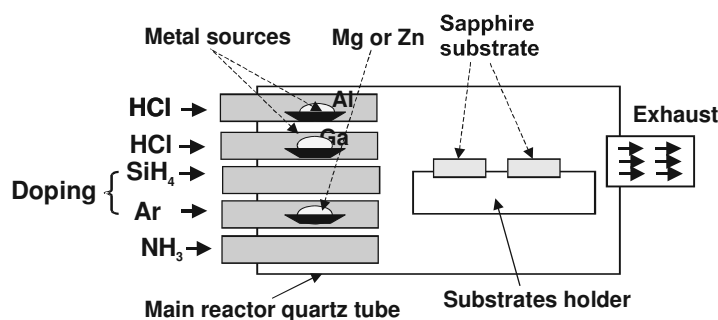


Fig. 3. Schematic of HVPE growth reactor used for experimental work.

### 3. Material Properties

#### 3.1. Undoped GaN Layers

GaN layers having thickness from 2 to 100  $\mu\text{m}$  and 0.1 to 2  $\mu\text{m}$  were grown on 2-inch sapphire and silicon carbide (SiC) substrates,

respectively. The growth was performed on (0001) c-plane sapphire or (0001)Si face of 6H- and 4H-SiC substrates. The upper thickness limit reflects cracking problem, which is more severe for SiC substrates.

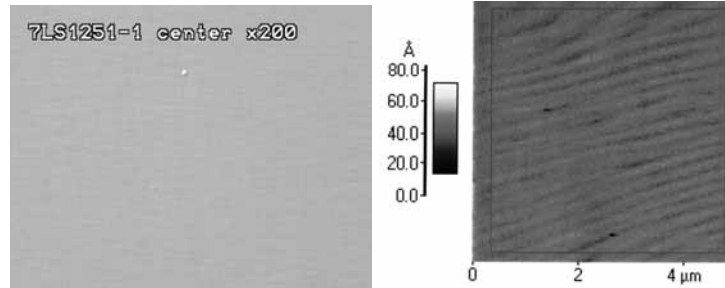


Fig. 4. Optical photo of 20  $\mu\text{m}$  thick GaN layer (left) and AFM image for 100  $\mu\text{m}$  GaN layer (right) grown on sapphire by HVPE (courtesy of Prof. S. Nikishin).

Surface of grown GaN layers was smooth and mirror like. Typical surface roughness, RMS, even for thick layers grown on sapphire was less than 0.5 nm (Fig. 4). For the smoothest layers, as-grown surface had RMS values below 0.2 nm. Characterization performed using reflectance high energy electron diffraction (RHEED) indicated that as-grown GaN surface is single crystal (Fig. 5).



Fig. 5. RHEED image for as grown GaN surface measured after air exposure.

Crystal structure of grown layers was investigated using x-ray diffraction methods. Typically crystal quality of the layers grown on sapphire improves with layer thickness. For layers thicker than 20  $\mu\text{m}$ ,

the full width at a half maximum (FWHM) values of x-ray diffraction  $\omega$ -scan rocking curves measured for GaN (00.2) and (10.2) reflections were less than 200 arcsec and 300 arcsec, respectively (Fig. 6). Dislocation density measured by transmission electron microscopy (TEM) for GaN grown on sapphire was about  $(1-3) \times 10^8 \text{ cm}^{-2}$  for 10  $\mu\text{m}$  thick layer.

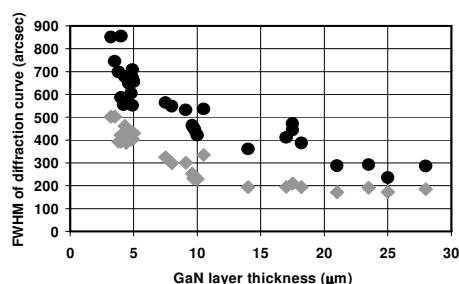


Fig. 6. The FWHM values of x-ray  $\omega$ -scan rocking curves measured for GaN layers with various thicknesses. The layers were grown by HVPE on sapphire substrates: diamonds correspond to the (00.2) reflections and circles correspond to the (10.2) reflections.

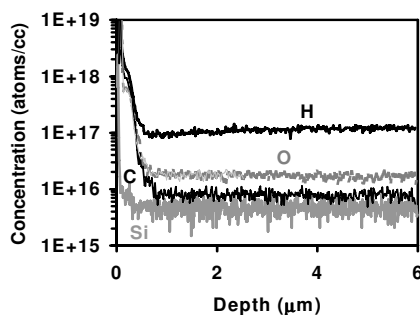


Fig. 7. SIMS depth profile for H, O, C, and Si impurities in undoped GaN layer grown on sapphire by HVPE.

For GaN layers grown on SiC, x-ray rocking curve FWHM values ranged from about 70 to 200 arc sec and from 200 to 800 arc sec for the (00.2) and the (10.2) reflections, respectively. Etch pit density for about 2  $\mu\text{m}$  thick GaN layer grown on SiC substrate was in a mid  $10^7 \text{ cm}^{-2}$  range. Crystal structure of thin GaN layers grown on SiC was described in the Ref.<sup>17</sup> P-n heterojunctions diodes formed by HVPE grown n-GaN

and p-SiC substrates were studied.<sup>18</sup> Properties of n-n and p-n GaN/SiC diodes have also been reported.<sup>19</sup>

Impurity contamination for undoped GaN layers was studied by means of SIMS. Results of SIMS measurements showed that background impurity concentrations are typically less than  $5 \times 10^{16} \text{ cm}^{-3}$ . SIMS impurity depth profiles for undoped GaN layer grown on sapphire are given in Fig. 7 show silicon, oxygen, hydrogen, and carbon atomic concentrations of about  $5 \times 10^{15}$ ,  $2 \times 10^{16}$ ,  $1 \times 10^{17}$ , and  $8 \times 10^{15} \text{ cm}^{-3}$ , respectively. Concentrations of background metallic impurities were also below  $10^{15} \text{ cm}^{-3}$  level as determined by SIMS and glow discharge mass analysis (Table 1). A concentration of electrically active non-compensated donors,  $N_D - N_A$ , measured for undoped GaN layers typically was below  $5 \times 10^{16} \text{ cm}^{-3}$ . Data collected for over a year time period for several HVPE growth machine are summarized in Fig. 8.

Table 1. Background impurity concentrations measured in undoped GaN layers by glow discharge mass analysis.

Element	Concentration [ppm wt]	Concentration [at/cm <sup>3</sup> ]	Element	Concentration [ppm wt]	Concentration [at/cm <sup>3</sup> ]
B	< 0.005	< 1.7E+15	Zn	< 0.01	< 5.7E+14
Mg	< 0.005	< 7.6E+14	Ge	< 0.1	< 5.1E+15
Si	0.08	1.1E+16	Se	< 0.01	< 4.7E+14
P	< 0.01	< 1.2E+15	Y	< 0.005	< 2.1E+14
Ca	< 0.05	< 4.6E+15	Mo	< 0.005	< 1.9E+14
Ti	< 0.005	< 3.9E+14	Cd	< 0.01	< 3.3E+14
V	< 0.005	< 3.6E+14	In	< 0.01	< 3.2E+14
Cr	< 0.005	< 3.6E+14	Sb	< 0.005	< 1.5E+14
Mn	< 0.01	< 6.7E+14	Te	< 0.005	< 1.5E+14
Fe	< 0.005	< 3.3E+14	W	< 0.005	< 1.0E+14
Co	< 0.005	< 3.1E+14	Re	< 0.005	< 9.9E+13
Ni	< 0.005	< 3.2E+14	Bi	< 0.005	< 8.9E+13

Most values of the concentration  $N_D - N_A$  ranges from  $2 \times 10^{15}$  to  $2 \times 10^{16} \text{ cm}^{-3}$  irrespective on the layer thickness. The data points being close to

$10^{17} \text{ cm}^{-3}$  range were caused probably by some accidental contamination. The  $N_D-N_A$  values in the  $10^{14} \text{ cm}^{-3}$  range may be originated by uncontrollable compensation. In general, for GaN layers thicker than  $3 \mu\text{m}$  no dependence of the concentration  $N_D-N_A$  on the layer thickness was detected. On the other hand, material crystal quality improvement with layer thickness is obvious. We may suggest that background electrical active shallow centers in grown undoped GaN are not related to crystal structure defects. Electron mobility and concentration determined by Hall measurements at room temperature for  $26 \mu\text{m}$  thick undoped GaN layer grown on sapphire was about  $760 \text{ cm}^2/\text{V sec}$  and  $4 \times 10^{16} \text{ cm}^{-3}$  (Fig. 9), respectively.

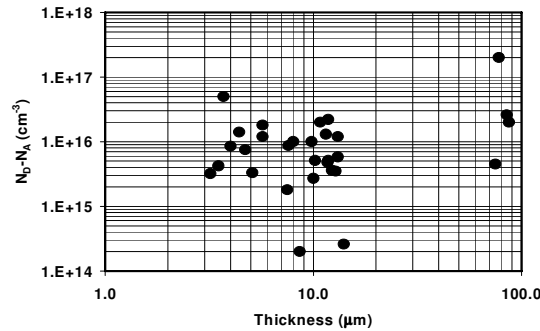


Fig. 8. Concentrations  $N_D-N_A$  for undoped GaN layers grown on sapphire substrates.

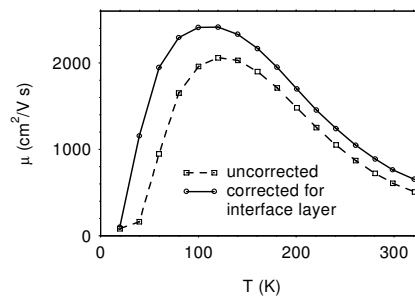


Fig. 9. Electron mobility measured by Hall method for  $26 \mu\text{m}$  thick GaN layer grown on sapphire. The data are corrected for highly conducting GaN/sapphire interface layer (courtesy of Prof. D. Look).

Optical properties of undoped GaN layers grown on sapphire were evaluated by photoluminescence (PL). For  $26 \mu\text{m}$  thick GaN layer the

near band PL peak had the FWHM of about 1.7 meV at 6 K (Fig. 10). For about 1  $\mu\text{m}$  thick GaN layers grown on SiC, the near band edge PL peak was located at 3.384eV (300 K) and 3.439 eV (77 K) and had the FWHM of 23 meV and 58 meV at 77 K and 300 K, respectively.

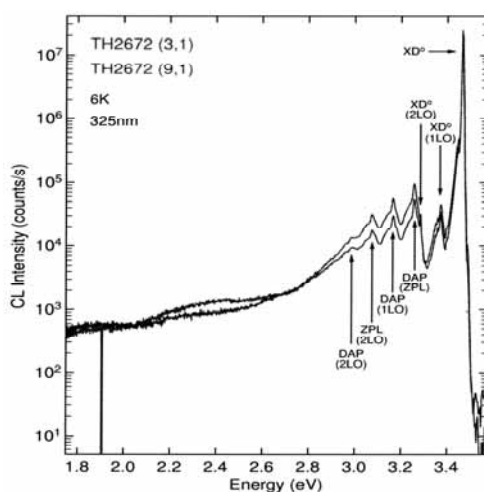


Fig. 10. Photoluminescence spectra for GaN layer grown on sapphire substrates. Two lines represent measurements made at two different locations on the sample. The FWHM for the  $X_A D^0$  peak is about 1.73 meV (courtesy of Dr. J. Freitas, Jr.).

### 3.2. Si-doped GaN Layers

Silicon is well known donor in GaN and is widely used to control n-type conductivity of GaN and AlGaN materials. By varying silane gas flow we controlled concentration  $N_D - N_A$  in HVPE grown GaN layers from  $1 \times 10^{17}$  to  $8 \times 10^{18} \text{ cm}^{-3}$ . Si depth profile measurements were performed by SIMS for HVPE grown epitaxial structure having five GaN layers (Fig. 11). The first and fifth (top) layers are undoped. Three intermediate layers were grown with various Si doping levels. It is clearly seen that Si doped layers have sharp interfaces.

Due to small activation energy of Si donor, at room temperature concentration  $N_D - N_A$  is almost equal to electron concentration. Electron Hall mobilities of about 312 and 214  $\text{cm}^2/\text{V sec}$  were measured at 300 K

for the materials having electron concentration of about  $1 \times 10^{18}$  and  $4 \times 10^{18} \text{ cm}^{-3}$ , respectively.

Crystal quality of highly Si doped ( $>10^{18} \text{ cm}^{-3}$ ) GaN layers are slightly deteriorated in comparison to undoped GaN layers. Another issue related to high Si doping is crack formation. Typically thickness for crack free highly Si doped GaN layers is kept below  $10 \mu\text{m}$ .

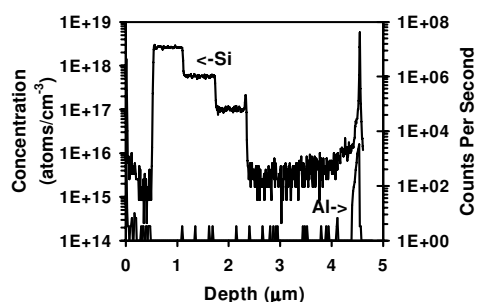


Fig. 11. Si depth distribution measured by SIMS in an HVPE-grown GaN epi structure comprising Si doped layers. The sample surface is on the left. The Al profile is shown to indicate the GaN-sapphire interface. Initial undoped GaN layer is about  $2 \mu\text{m}$  thick.

### 3.3. Mg-doped GaN Layers

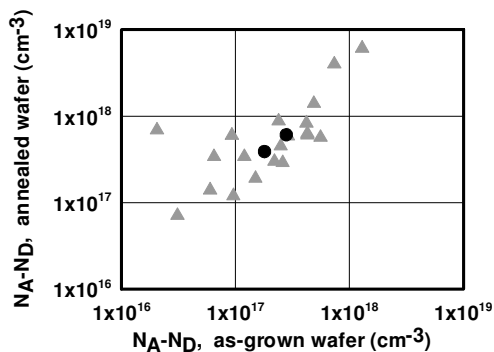


Fig. 12. Concentration  $N_A - N_D$  after annealing vs. concentration  $N_A - N_D$  for as-grown samples: Mg-doped (triangles) and Zn-doped (circles) GaN layers.

Mg doping<sup>20</sup> resulted in the demonstration of the first HVPE grown p-type GaN layers and pn junctions. Thickness of p-GaN layers ranged from 3 to  $5 \mu\text{m}$ . As grown Mg doped GaN layers had p-type conductivity

with concentration  $N_A-N_D$  up to  $2 \times 10^{18} \text{ cm}^{-3}$ . After sample anneal at  $750^\circ\text{C}$  in argon ambience for 40 min an increase of the concentration  $N_A-N_D$  in 1.5-3 times was detected (Fig. 12). One possible explanation of high p-type doping measured for as-grown GaN layers is low hydrogen concentration in HVPE grown GaN layers.

Hydrogen is known to form H:Mg complex in GaN and post-growth thermal treatment (annealing) is required to withdraw H from the complex and to obtain p-type conductivity for MOCVD grown materials. Note that in MOCVD technology hydrogen is used as a carrier gas and present in large concentration in the growth zone. Besides hydrogen, threading defects can bond Mg atoms that also prevent p-type material fabrication. Developed HVPE process is free of the hydrogen gas (except of small amount of hydrogen produced by ammonia decomposition). Argon is used as a carrier gas in TDI HVPE processes. Thus, good crystalline quality and lower hydrogen concentration explain high p-type conductivity of as grown Mg-doped GaN layers fabricated by HVPE.

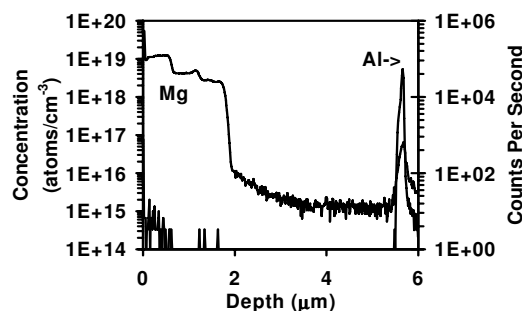


Fig. 13. Mg depth distribution measured by SIMS in an HVPE-grown Mg-doped GaN layer. As grown sample had p-type conductivity. The Al profile is shown to indicate the GaN-sapphire interface. Undoped part of the structure is about  $3.5 \mu\text{m}$  thick.

Good control for Mg doping was proved by SIMS measurements (Fig. 13). The studied structure consists of undoped  $3.5 \mu\text{m}$  thick GaN layer deposited on sapphire substrate and three subsequently grown Mg-doped GaN layers with increasing doping concentration toward the structure surface. All four layers were grown in the same HVPE run.

The SIMS profiling demonstrates ability of HVPE technique to fabricate abrupt Mg doping profiles during GaN growth. Recent Mg doping experiments<sup>21</sup> resulted in p-type GaN layers showing hole mobility of  $80 \text{ cm}^2/\text{V sec}$  at hole concentration of  $1 \times 10^{18} \text{ cm}^{-3}$  at room temperature. These results present record high carrier mobility for p-type GaN and must be further investigated.

The FWHM values for XRD rocking curves measured for Mg doped samples were slightly larger than the ones for undoped and Si doped samples ranging from 350 to 410 arc sec and from 600 to 800 arc sec for symmetric (00.2) and asymmetric (10.2) reflections, respectively.

Highly Mg doped GaN layers have been applied to form blue and UV LEDs by HVPE technology (Section 5).

### 3.4. Zn-doped GaN Layers

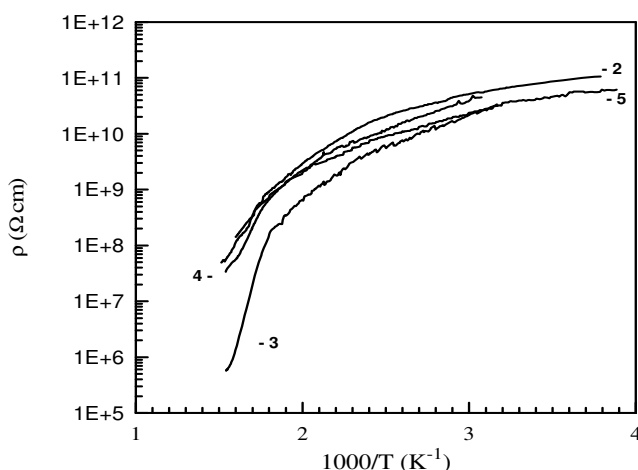


Fig. 14. Temperature dependence of electrical resistivity measured in several locations for semi insulating GaN compensated with Zn. The layer was grown on conductive SiC substrate.

GaN doping with Zn during HVPE growth has been widely used for formation of light emitting and photo detector device structures.<sup>3</sup> In these structures Zn-doped layers were semi insulating. We have fabricated

semi insulating Zn-doped GaN layers grown by HVPE on SiC substrate (Fig.14) and sapphire substrates. Grown materials demonstrated room temperature electrical resistivity above  $10^{10}$  Ohm cm.<sup>22</sup>

Detailed study of Zn doping showed that by controlling Zn vapor pressure in the growth zone it is possible to fabricate three basic structures: (1) n-type GaN layers compensated with Zn, (2) semi-insulating Zn-doped layers, and, surprisingly, (3) p-type GaN layers doped with Zn. The first p-type GaN doped with Zn has been reported by Polyakov et al.<sup>23</sup>. For p-type GaN layers doped with Zn a maximum concentration  $N_A-N_D$  of about  $6 \times 10^{17}$  cm<sup>-3</sup> was measured (Fig. 12). We believe that p-type doping of GaN with Zn is due to low background impurity concentration and low defect density in HVPE grown layers. More information of two-dimensional hole gas detected in p-type Zn doped GaN/AlGaIn structures is given in Section 4.

### 3.5. AlN Layers

HVPE growth of AlN layers is studied substantially less than that for GaN layers. In 1972, Yim and co-workers grew AlN on sapphire substrates in the temperature range 1000-1100°C by HVPE method where AlCl<sub>3</sub> was generated by passing HCl over molten aluminum.<sup>2</sup> However, results on HVPE growth of AlN are limited.<sup>24,25, 26</sup>

Recently, we demonstrated HVPE growth technology for thick AlN layers. The first free-standing AlN wafers were fabricated by growing up to 1 mm thick AlN layers on silicon substrates and subsequent removal of the substrate by chemical etching.<sup>27</sup> Properties of free-standing AlN wafers fabricated by HVPE are given in Section 5.

Lately, HVPE technology has been modified to deposit high quality thin AlN and AlGaIn epitaxial layers on SiC<sup>28, 29</sup> and sapphire substrates.<sup>30</sup> AlN layers were deposited on (0001)Si on-axis surface of SiC substrates. Thickness of AlN layer was varied from 0.1 to 0.7 microns. Surface roughness, RMS measured by AFM ranged from 1 to 5 nm. RHEED measurements showed that grown AlN layers have single crystal surface meaning that air exposure does not result in a formation of thick amorphous oxide layer. X-ray diffraction study indicated high

crystal quality of the grown layers having a minimum FWHM value of  $\omega$ -scan (0002) rocking curve of about 80 arc sec. Specific electrical resistivity of AlN exceeded  $10^{11}$  Ohm cm at room temperature (Fig. 15).

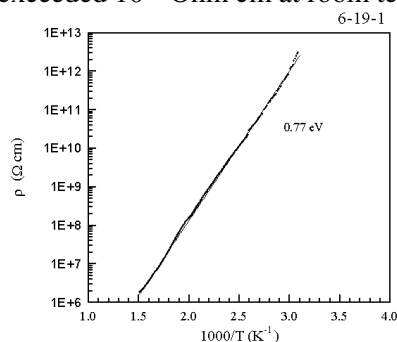


Fig. 15. Temperature dependence of electrical resistivity for semi insulating undoped AlN layer grown on SiC substrate.

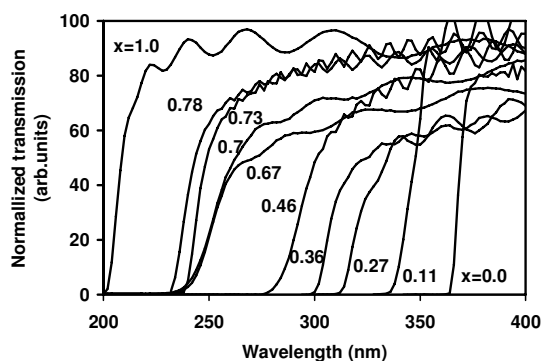


Fig. 16. Optical transmission spectrum for AlN/sapphire, GaN/sapphire and Al<sub>x</sub>Ga<sub>1-x</sub>N (0.11 < x < 0.78)/sapphire epitaxial wafers grown by HVPE.

Cathodoluminescence measurements performed at room temperature on thin AlN layers grown on SiC substrates revealed near band edge luminescence peaking at 5.9 eV. Device structures based on HVPE grown thin AlN and AlGa<sub>x</sub>N layers are described in Section 5.

Thin (<1 μm) AlN layers with mirror like surface were grown on sapphire substrates. However AlN surface was rougher than that for GaN layers. Surface roughness, RMS for AlN on sapphire ranged from 3 to 15

nm. Grown AlN/sapphire samples exhibited good optical transparency in UV spectrum region (Fig. 16).

Relatively narrow x-ray (00.2) AlN  $\omega$ -scan rocking curves with the FWHM values of about 80 arc sec were measured for several samples, but for such samples the asymmetric (10.2) x-ray rocking curves were much wider with the FWHM values exceeding 1500 arc sec. The narrowest (10.2) x-ray  $\omega$ -scan rocking curve measure so far for thin AlN layer grown on sapphire had the FWHM of 310 arc sec with the FWHM for the (002) peak of 177 arc sec. Currently, HVPE process for low defect thin AlN layers on sapphire is under development.

Thick (> 5 microns) crack-free AlN layers were grown on 2-inch and 3-inch SiC and sapphire substrates by stress control HVPE method<sup>31</sup>. Thickness of grown AlN layers ranged from 1 to 20 microns for material grown on sapphire and from 5 to 75 microns for material grown on SiC. Both 6H- and 4H-SiC wafers were used as substrates. The layers were deposited on (0001)Si face of SiC wafers and on (0001) c-plan of sapphire wafers. Surface of AlN layers had characteristic pyramidal relief with RMS roughness ranging from 20 to 70 nm. After polishing, AlN surface had roughness less than 0.5 nm. The minimum FWHM values for the (002) AlN  $\omega$ -scan x-ray rocking curves were about 250 arc sec and 500 arc sec for layers grown on SiC and sapphire substrates, respectively. Wet chemical etching of thick AlN layers grown on SiC resulted in etch pit density ranging from mid  $10^7$  cm<sup>-2</sup> to low  $10^8$  cm<sup>-2</sup>. 2-inch diameter AlN free standing wafers were fabricated by removing SiC substrate by reactive ion etching (Section 5).

### 3.6. AlGa<sub>N</sub> Layers

Initial results on HVPE grown AlGa<sub>N</sub> alloys were reported in the 70<sup>th</sup><sup>4</sup>. In that study Ga and Al were transported to a reaction zone as subchlorides by passing HCl diluted with nitrogen gas over a mixed melt of Ga and Al in a graphite boat. Sapphire substrates had the (21-31) orientation resulted in (11-20) AlGa<sub>N</sub> films. Composition of the grown layers was varied from 0 to 100 mol. % AlN by controlling Ga to Al ratio in the source material. Cathodoluminescence and optical absorption of grown materials were studied for entire composition range. Electrical

properties of HVPE grown AlGa<sub>x</sub>N alloy layers having AlN content up to 45 mol. % were studied<sup>33</sup> showing background electron carrier concentration in the  $10^{19} \text{ cm}^{-3}$  range, which decreased as AlN content increases. Recently, up to 75  $\mu\text{m}$  thick AlGa<sub>x</sub>N layers were grown on sapphire by HVPE using mixed Ga+Al sources.<sup>34</sup>

To deposit AlGa<sub>x</sub>N layers by HVPE we used separate Ga and Al metal sources. The whole composition range of AlGa<sub>x</sub>N alloys was covered by controlling a ratio of aluminum and gallium chlorides partial pressures in the growth zone (Fig. 17). Composition of AlGa<sub>x</sub>N layers was determined using x-ray diffraction data assuming that Vegard's law is valid. The experimental uncertainty in that determination of the Al<sub>x</sub>Ga<sub>1-x</sub>N composition was estimated to be  $x \sim 0.02$ . Composition for grown alloy epitaxial layers was reasonably uniform across the wafer (Fig. 18).

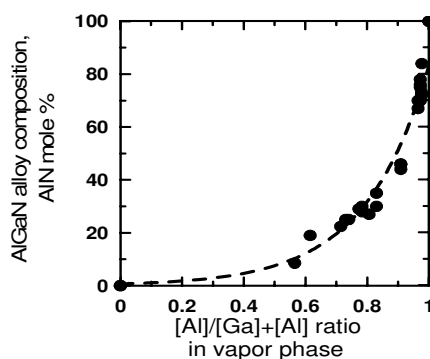


Fig. 17. Vapor phase-solid phase composition diagram for HVPE grown AlGa<sub>x</sub>N alloys.

Best 2-inch wafers had standard deviation for AlN composition of about 1 mole % of AlN. Typical thickness of crack-free AlGa<sub>x</sub>N layers grown on sapphire substrates ranged from 0.3 to 2  $\mu\text{m}$ . The FWHM of XRD rocking curves changes with AlGa<sub>x</sub>N composition attaining the lowest values of 350 arcsec and 1400-1800 arcsec for the (00.2) symmetric and the (10.2) asymmetric reflections, respectively for high range of Al<sub>x</sub>Ga<sub>1-x</sub>N composition ( $0.65 < x < 0.85$ ). Minimum estimated screw and edge dislocation densities in AlGa<sub>x</sub>N layers were  $< 6 \times 10^8 \text{ cm}^{-2}$  and  $< 2 \times 10^9 \text{ cm}^{-2}$ , respectively. For undoped Al<sub>x</sub>Ga<sub>1-x</sub>N layers grown on sapphire, background concentration  $N_D - N_A$  depended on alloy

composition  $x$ . For  $x < 0.3$ , AlGa<sub>x</sub>N layers show n-type conductivity and concentration  $N_D - N_A$  is in  $10^{17} - 10^{18} \text{ cm}^{-3}$  ranges. Hall measurements showed electron mobility of about  $166 \text{ cm}^2/\text{V sec}$  and electron concentration of  $9 \times 10^{17} \text{ cm}^{-3}$  (300 K) for alloy having 18 mol. % of AlN. For  $x$  values near 0.5 or larger, Al<sub>x</sub>Ga<sub>1-x</sub>N materials were almost insulating and correct C-V measurements were not possible.

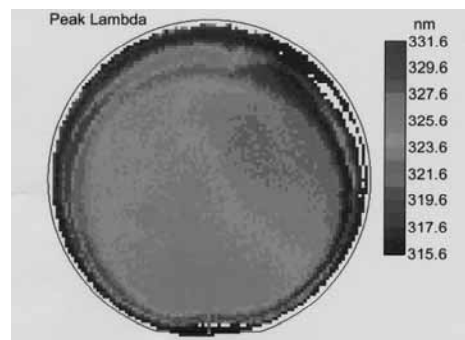


Fig. 18. Photoluminescent map for 2-inch AlGa<sub>x</sub>N-on-sapphire epitaxial wafer. Standard peak lambda deviation is 0.65%. Average AlGa<sub>x</sub>N composition is about 16 AlN mole % (courtesy of Accent Optical Technologies).

Normalized optical transmission spectra of crack-free HVPE-grown Al<sub>x</sub>Ga<sub>1-x</sub>N layers are shown in Fig. 16. The interference fringes appeared on the transmission curves at the wavelengths longer than cut-off wavelength indicate smooth surfaces of these AlGa<sub>x</sub>N layers. At 265 nm optical transmission of 71% and 73% was measured for Al<sub>x</sub>Ga<sub>1-x</sub>N layers having composition of  $x \sim 0.73$  and  $x \sim 0.78$ , respectively. Energy gap,  $E_g$ , obtained from transmission measurement found to correlate with the PL peak position that can be ascribed to near-band-edge recombination in the layer grown. The transmission and PL data are collected together in Fig. 19 to plot optical band-gap energy of Al<sub>x</sub>Ga<sub>1-x</sub>N alloys as a function of composition  $x$  (AlN mole fraction).

The  $E_g$  values for undoped GaN layer defined from absorption and PL measurements, corresponded well to each other within  $\pm 10 \text{ meV}$  accuracy range, were equal to 3.41 eV. For AlN band-gap energy was found to be 6.13 eV. Dotted line is linear interpolation between  $E_{g\text{GaN}}$

(3.4 eV) and  $E_{g_{AlN}}$  (6.1 eV). Solid line was calculated using  $E_g = xE_{g_{AlN}} + (1-x)E_{g_{GaN}} - bx(1-x)$  equation with bowing parameter  $b=1.1$  eV. Refractive index of AlGa<sub>1-x</sub>N layers grown by HVPE was studied in the Ref.<sup>35</sup> Undoped AlGa<sub>1-x</sub>N layers grown by HVPE on SiC substrates were described in ref.<sup>36, 37</sup> Doping of AlGa<sub>1-x</sub>N alloys grown by HVPE is not investigated in details yet. The fact that AlGa<sub>1-x</sub>N/AlGa<sub>1-x</sub>N p-n heterostructures are working as 300 nm UV light emitters<sup>38</sup> indicates that p-type doping is possible at least up to 27 mol. % of AlN. We may conclude that AlN and AlGa<sub>1-x</sub>N epitaxial layers can be grown by HVPE with a reasonable composition control and crystal quality. However, HVPE growth of AlGa<sub>1-x</sub>N and AlN layers is investigated much less than HVPE growth of GaN.

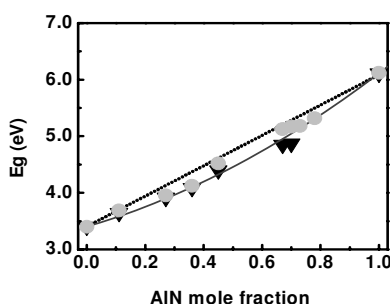


Fig. 19. Dependence of Al<sub>x</sub>Ga<sub>1-x</sub>N optical band gap on AlN mole fraction ( $x$ ) derived from room temperature photoluminescence (triangles) and optical transmission data (circles).

### 3.7. InN and InGa<sub>1-x</sub>N Layers

Results on HVPE growth of InN and InGa<sub>1-x</sub>N materials are limited. The first deposition process was performed more than 25 years ago when InN epitaxial layers were grown using reaction between ammonia and InCl<sub>3</sub><sup>39</sup>. InCl<sub>3</sub> was synthesized in a separate experiments from In and Cl<sub>2</sub>. The layers were deposited on sapphire and quartz substrates. Deposition rate ranged from 1 to 8  $\mu$ m per hour depending on growth conditions. Source temperature and substrate temperature were controlled from 200 to 600°C and from 450 to 700°C, respectively. The maximum growth rate was observed at 600°C. Grown materials had n-type conductivity with

electron concentration from  $2 \times 10^{20} \text{ cm}^{-3}$  to  $8 \times 10^{21} \text{ cm}^{-3}$  and mobility 35 – 50  $\text{cm}^2/\text{V s}$ .

Later several research teams reported HVPE growth of InN-containing materials<sup>40,41</sup>. Thermodynamics of HVPE growth process for InGaN layers was analysed in the Ref.<sup>42</sup>. InN growth using InCl and InCl<sub>3</sub> sources was reported.<sup>43,44</sup> InGaN alloy layers were grown employing InCl<sub>3</sub>, GaCl<sub>3</sub> and NH<sub>3</sub> sources.<sup>45</sup> When InCl-NH<sub>3</sub> material system was used, very low growth rate (<0.05  $\mu\text{m/hr}$ ) was observed. In contrast, use of InCl<sub>3</sub>-NH<sub>3</sub> material source system resulted in InN growth rate up to 0.3  $\mu\text{m/hr}$ . The growth rate obtained at 750°C was about 0.2  $\mu\text{m/hr}$ . The minimum FWHM value of x-ray rocking curve of about 24.7 arc min was measured for InN grown at 700°C.

Growth of InGaN thin films by HVPE was reported in ref.<sup>46</sup>. In that work, separate sources of metal Ga and In were placed in a single HCl gas channel to form gallium and indium chlorides. The composition of alloy InGaN layers was controlled by varying the ratio of the effective metal surface areas in the range from 0.3 to 35 (In/Ga).

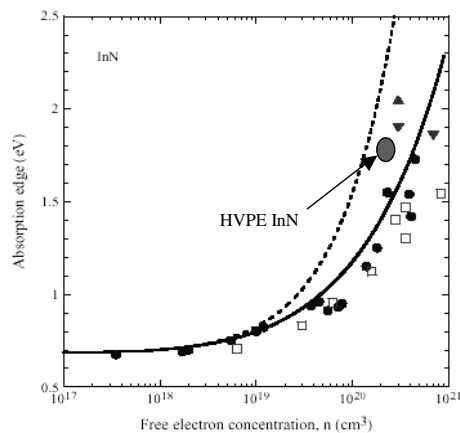


Fig. 20. The energy of the optical absorption edge as a function of the free electron concentration in InN material grown by different techniques (after J. Wu, W. Walukiewicz<sup>48</sup>). Position of TDI InN HVPE grown material is shown.

Recently, our team has reported novel results on HVPE growth of InN materials and heterostructures.<sup>47</sup> The growth was performed on 2-

inch sapphire substrates and also on GaN/sapphire, AlN/sapphire, and AlGaIn/sapphire templates (Fig. 20). Growth temperature was varied from 500 to 700°C. For continuous InN layers, thickness ranged from 0.3 to 2 microns. X-ray diffraction rocking curves measured using  $\omega$ -scanning geometry for the (00.2) InN reflection had the FWHM of about 460 arc sec for continuous InN layers.

It was observed that depending on growth conditions, InN materials may be grown as continuous layers or nano-size structures. The nano-structures had shape of nano-rods or nano-wires with a typical diameter of about 60 - 500 nm and length ranging from a few hundred nanometers to a few microns (Fig. 21). Investigation of InN HVPE process and materials is under way.

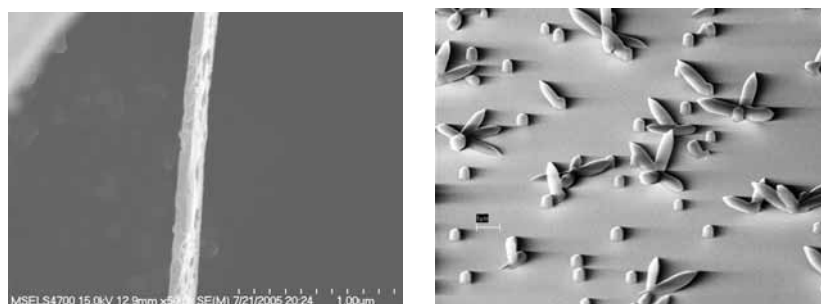


Fig. 21. SEM photographs of GaN nano wire (left) and nano-size InN structures (right) grown on sapphire (courtesy of Dr. A. Davydov and Prof. S. Nikishin). Image width is about 2  $\mu\text{m}$  for top picture and about 16  $\mu\text{m}$  for bottom picture.

## 4. New Directions in HVPE Development

### 4.1. Large Area and Multi Wafer HVPE Growth

Novel HVPE growth equipment developed at TDI, Inc. allowed us to grow GaN, AlN, and AlGaIn layers and multi-layer structures on large area (>2-inch) substrates, for the first time. GaN layers grown on 4-inch sapphire substrates showed material parameters similar to that for 2-inch diameter samples. Interestingly, undoped GaN layers grown on 4-inch

sapphire showed some reduction of  $N_D-N_A$  concentration being in high  $10^{14} \text{ cm}^{-3}$  to low  $10^{15} \text{ cm}^{-3}$  range. Typical standard thickness deviation for GaN layers grown on 4-inch substrates was about 5 %. Uniform n-type doping was achieved for Si-doped GaN layers grown on 4-inch sapphire with electrical resistivity uniformity better than 5 %. Recently, AlN and GaN layers were successfully grown on 6-inch diameter Si and sapphire substrates, respectively (Fig. 22). These results demonstrate ability of HVPE process and equipment to handle large size epitaxial structures.

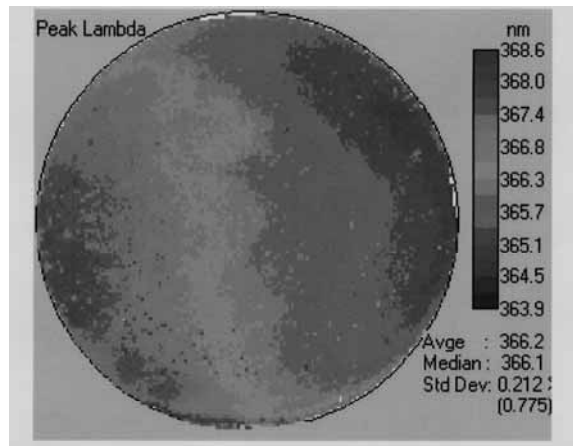


Fig. 22. Photoluminescence map for 6-inch GaN-on-sapphire epitaxial wafer (courtesy of Accent Optical Technologies). Standard deviation of peak PL wavelength for the whole wafer is 0.2 %.

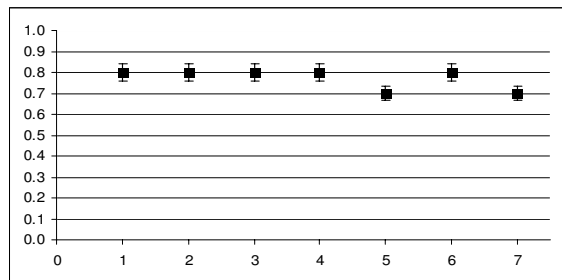


Fig. 23. Thickness of seven AlGaIn layers grown on 2-inch sapphire substrates in the same HVPE process. The layer thickness was measured in the wafer centre.

Another direction of the development of HVPE production technology is design of multi wafer HVPE growth machines and processes. Such machines existing for HVPE growth of other compound semiconductor have not been developed for GaN materials until recently. TDI, Inc. is developing and putting in operation HVPE machines with large wafer capacity to reduce manufacturing cost. Novel HVPE equipment is capable to carry out simultaneous growth seven 2-inch (7×2") wafers (Fig. 23), or 3×3" wafers, or 2×4" wafers and further scaling of the equipment and process is under way.

#### 4.2. Multi-layer Structures

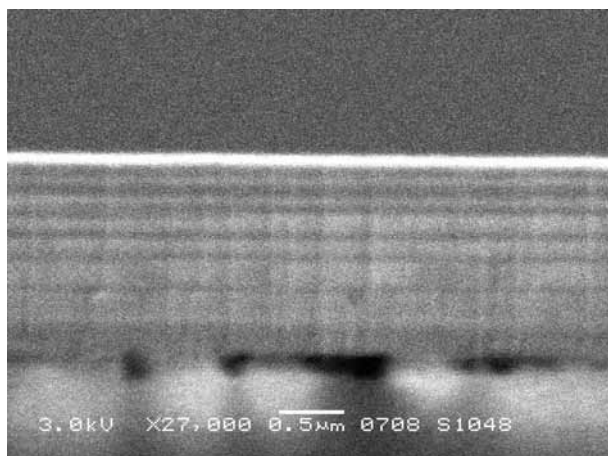


Fig. 24. SEM image of cleaved edge of multi layer AlGaIn/GaN epitaxial structure grown on sapphire substrate. Dark regions and light regions corresponds GaN and AlGaIn layers, respectively.

Multi layer HVPE growth of GaN-based structures has been used to fabricate M-I-S light emitting structures in the 1970<sup>th</sup>.<sup>49</sup> Recently, novel avenue for nitride HVPE has been opened by the demonstration of controllable growth of nm-thick layers and fabrication multi-layer structures. Growth rate of GaN and AlGaIn layers was controlled below 2 μm/hr making it possible to fabricate multi layer structures with sub-micron layers. Equipment and process were modified to grow

GaN/AlGaN heterostructures with sharp interfaces. One example of such multi-layer AlGaN/GaN is demonstrated in Fig. 24.

Thickness of different AlGaN and GaN layers in this structure was controlled from about 20 to 260 nm and 50 – 250 nm, respectively, by varying growth time for each layer.

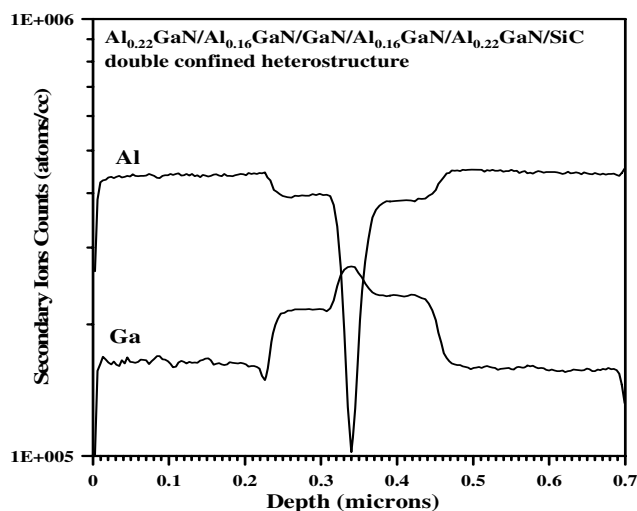


Fig. 25. SIMS element depth profiles for AlGaN/GaN/AlGaN double heterostructure grown by HVPE on SiC substrate.<sup>29</sup>

SIMS depth analysis of another HVPE grown AlGaN/GaN/AlGaN double heterostructure is given in Fig. 25. GaN well was of about 20 nm thick. Stimulated emission under optical pumping conditions was observed from this structure at room temperature at a wavelength of 370 nm with a threshold of about  $540 \text{ kW/cm}^2$ .<sup>29</sup>

### 4.3. P-n Junctions

Two-layer GaN pn-structures were fabricated by *in-situ* p-type doping during HVPE growth.<sup>20</sup> First, undoped GaN layer was grown directly on 6H-SiC substrate. Then Mg was introduced as an acceptor dopant to grow p-type GaN layer. The Mg atomic concentration ranged for different samples from  $5 \times 10^{19}$  to  $5 \times 10^{20} \text{ cm}^{-3}$ . Mesa diodes with a

vertical current flow geometry were formed by reactive ion etching. Current-voltage and capacitance-voltage characteristics of the p-n diodes indicating good rectifying properties were measured.

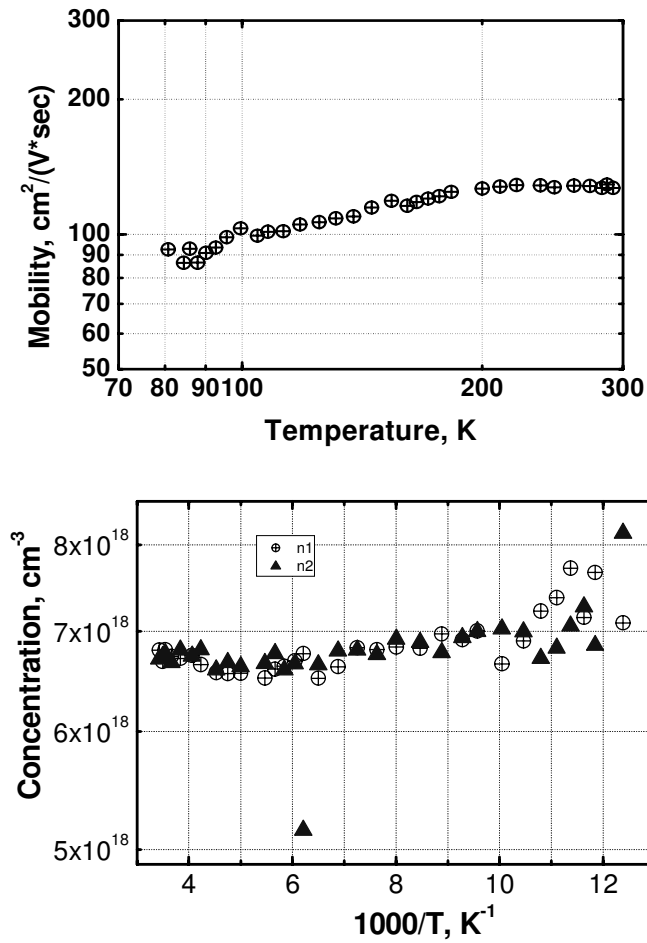


Fig. 26. Temperature dependencies of hole mobility (top) and hole concentration (bottom) measured for p-type GaN/AlGaIn hetero structure with 2DHG.<sup>21</sup> Triangles and dots represent data measured at different locations on the sample.

The electroluminescence from the p-n diodes peaking at 420 nm was detected. These results have demonstrated an ability of HVPE

technology to form GaN-based structures for optoelectronic devices (Section 5).

#### **4.4. Structures with Two Dimensional Carrier Gas**

Another example of multi layer structures grown by HVPE is AlGaN/GaN heterostructures with two dimensional electron gas (2DEG).<sup>50</sup> These structures were grown on sapphire substrates. Thickness of GaN and AlGaN layers were 3  $\mu\text{m}$  and 25 nm, respectively. AlN concentration in the alloy layers was about 25 mol. %. The structures exhibited room temperature electron mobility of about 800  $\text{cm}^2/\text{V sec}$  at sheet charge density of about  $1 \times 10^{13} \text{ cm}^{-2}$ . At low temperature electron mobility up to 4000  $\text{cm}^2/\text{V sec}$  was measured. For p-type GaN/AlGaN structures formation of two dimensional hole gas (2DHG) was also detected (Fig. 26).<sup>21</sup> Hole mobility of 120  $\text{cm}^2/\text{V sec}$  at hole concentration of  $6 \times 10^{18} \text{ cm}^{-3}$  was measured at room temperature. Investigation and further development of epitaxial structures containing 2DHG may substantially benefit fabrication of GaN-based bipolar devices.

#### **4.5. Nano Structures and Porous Materials**

In this chapter we are focusing on continuous epitaxial layers and structures grown by HVPE. However, we would like to mention a fabrication of nanowires and nano rods by HVPE. Recently, GaN<sup>51</sup> and InN<sup>47</sup> nano structures (Fig. 21) have been demonstrated. Porous nano-size GaN materials were grown from single crystal continuous GaN layers by wet anodization.<sup>52, 53</sup> GaN growth on porous substrates resulted in stress and defect density reduction in grown epitaxial layers.<sup>54</sup> The nano size materials have an important meaning for future device applications.

Novel directions in group III nitride HVPE developments also include epitaxial overgrowth experiments to reduce defect density and GaN growth on non polar planes of sapphire substrates. However, these very interesting areas are out of scope of this chapter.

## 5. Applications of HVPE Grown Group III Nitride Materials

### 5.1. Substrate Applications

#### 5.1.1. Template substrates

The idea of template substrate comprising thin (from 0.5 to 100 microns) nitride layer on a foreign material, for example 10  $\mu\text{m}$  thick GaN on 2-inch sapphire, has been discussed in numerous publications.<sup>55, 56, 57</sup> Template substrates provide native GaN (AlN or AlGaN) surface for subsequent epitaxial growth. Buffer layer is not needed to form high quality nitride epitaxial layer/structure on template substrates. Various types of template substrates have been discussed in the literature include (1) low defect from 5 to 20  $\mu\text{m}$  thick n-type GaN-on-sapphire templates for high-power, high-brightness blue, green, and white LEDs, (2) p-type GaN-on-sapphire templates, (3) UV transparent AlGaN-on-sapphire templates for UV LEDs, (4) semi insulating i-GaN-on-sapphire templates for electronic devices, and (5) AlN-on-sapphire and AlN-on-SiC templates for high power high electron mobility transistors (HEMTs). HVPE is a method of choice to fabricate template substrates due to high growth rate, low defect density in grown materials, and relatively low cost of the technology.

Growth of group III nitride materials on template substrates was investigated using HVPE,<sup>58</sup> MOCVD<sup>59</sup> and MBE<sup>60, 61</sup> techniques. Defect density reduction and material quality improvements in homoepitaxial GaN layers grown on GaN template substrates have been demonstrated.<sup>30</sup> Template substrates have been successfully used for group III nitride optoelectronic and electronic<sup>32, 62, 63</sup> devices including blue LEDs on GaN/SiC templates<sup>64</sup> and GaN/sapphire templates.<sup>57</sup> Ultra violet (UV) AlGaN-based LEDs have been fabricated on UV transparent AlGaN/sapphire templates.<sup>66</sup> Laser diodes and high quality LEDs were made on HVPE grown templates with low defect density reached due to lateral overgrowth approach.<sup>67</sup> HVPE grown semi insulating GaN/sapphire and AlN/SiC templates have been used as substrates for

high frequency GaN-based HEMT devices.<sup>68</sup> Fabrication of template substrates by HVPE is technically and economically attractive due to high deposition rate and relatively low defect density in thick HVPE grown epitaxial layers. Definite advantage of template substrates is a possibility to use large size initial substrate such as 4-inch sapphire or 6-inch Si. The main technical challenges are relatively high defect density, cracking and substantial bowing of template substrates containing thick nitride layers. Some promising results on the bow control of AlN layers grown by HVPE on foreign substrates have been recently achieved by stress control HVPE method.<sup>31</sup>

#### 5.1.2. Free-standing substrates

30 mm diameter GaN free standing wafers have been reported in 1998.<sup>10</sup> Thick (up to 200  $\mu\text{m}$ ) GaN layers were grown by HVPE on 6H-SiC substrates. The SiC substrate was removed by reactive ion etching resulting in freestanding GaN wafer. These wafers exhibited very low defect density measured by TEM. Dislocation density was  $1 \times 10^7 \text{ cm}^{-2}$  and  $4 \times 10^5 \text{ cm}^{-2}$  for material located at 10 microns away and 100 microns away from GaN/SiC interface, respectively (Fig. 2).<sup>13</sup> Free standing GaN wafers have also been fabricated using HVPE growth of thick GaN layers on sapphire,<sup>70, 71</sup> LiGaO<sub>2</sub> substrates,<sup>72</sup> and GaAs substrates.<sup>73</sup> Typical dislocation density in GaN free standing wafers is in  $10^6 - 10^7 \text{ cm}^{-2}$  range. These GaN materials exhibited record high electron mobilities and very good optical properties. Properties of freestanding GaN wafers and their applications are described in numerous publications.<sup>65,69,74-78</sup>

AlN<sup>27</sup> and AlGa<sup>79</sup> freestanding wafers have also been reported. AlN free standing wafers were fabricated using Si and SiC initial substrates. Thick AlN layers were grown by HVPE and initial substrates were removed after HVPE growth. Mechanical<sup>80</sup>, electrical<sup>81</sup>, and structural<sup>13</sup> properties of free standing AlN crystals have been reported. AlN materials fabricated by HVPE using silicon initial substrates demonstrated record high thermal conductivity of  $3.3 \text{ WK}^{-1} \text{ cm}^{-1}$ <sup>82</sup> and high electrical resistivity ( $>10^{11} \text{ Ohm cm}$ , 300 K).<sup>81</sup> However, due to

significant lattice and thermal mismatch to initial Si substrate, dislocation density in grown AlN layers exceeded  $10^8 \text{ cm}^{-2}$  and corresponding x-ray rocking curves were relatively wide, of about 40 arc min for the rocking curves measured using  $\omega$ -scanning geometry for the (0002) AlN reflex.<sup>13</sup> Recently, 2-inch diameter freestanding AlN wafers have been fabricated using SiC initial substrates<sup>31</sup>, which were removed by reactive ion etching after HVPE deposition of thick AlN layers.

Free standing AlGaIn wafer<sup>79</sup> were fabricated by growing thick (up to 0.6 mm) undoped AlGaIn layer on SiC substrate and subsequent removal of the SiC substrate by reactive ion etching. AlN concentration in fabricated AlGaIn wafers was estimated of about 35 mol. %. The wafers demonstrated n-type conductivity with electron concentration in the  $10^{17} \text{ cm}^{-3}$  range. Currently, free-standing technology is the only commercial method to fabricate 2-inch GaN substrates with defect densities below  $10^7 \text{ cm}^{-2}$ . Laser diodes<sup>83, 84</sup> and LEDs have been fabricated on GaN free standing wafers.<sup>85</sup> High voltage M-I-M device structures were fabricated using free standing AlN wafers.<sup>81</sup> However, due to the fact that every wafer is fabricated from a thick epitaxial layer grown on a foreign substrate and, as a result, fabricated material is highly stressed and contains defects originated by heteroepitaxial growth, this approach has significant technical and economical limitations.

### 5.1.3. Bulk substrates

Recently HVPE-based bulk growth technologies were proposed to fabricate bulk GaN and AlN crystals.<sup>86</sup> The method involves growth of GaN boule on GaN seed, boule slicing, and wafer polishing (Fig. 27). High quality GaN homoepitaxial layers (Fig. 28) with defect density in the  $10^6 \text{ cm}^{-2}$  range and blue LEDs were fabricated on bulk GaN wafers. Although the bulk approach has very good potential for cost effective manufacturing of low defect large size GaN substrates, current size of demonstrated GaN boule is small and substantial development for this technology is needed. Bulk GaN technology based on HVPE approach is under development at several organizations.<sup>87, 88</sup>

Bulk AlN substrates were fabricated from AlN boules grown by a vapor transport technique based on HVPE technology.<sup>89</sup> AlN wafers up

to 1.75-inch diameter were sliced from single crystal AlN boules. Specific resistivity of the AlN bulk material was evaluated in the temperature range from 250 to 650 K. Material electrical resistivity exceeds  $10^8$  Ohm cm at room temperature and  $10^6$  Ohm cm at 500 K.

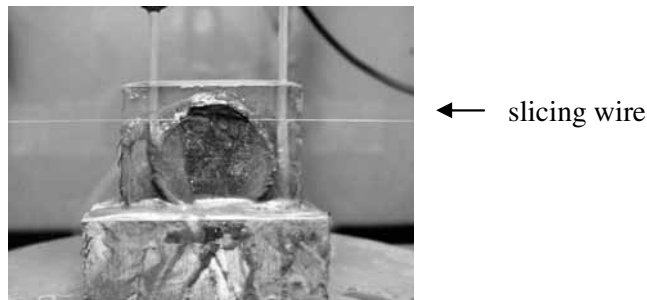


Fig. 27. Photo of 35 mm diameter GaN boule under diamond wire slicing. The boule was grown by modified HVPE technology at TDI, Inc.

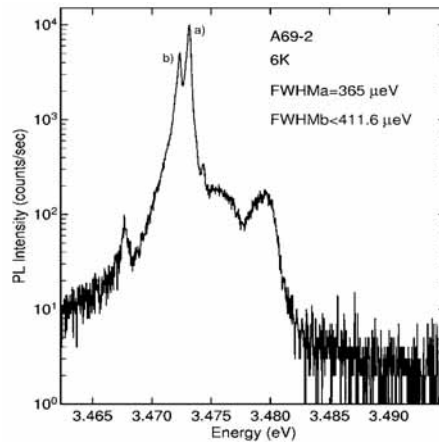


Fig. 28. PL spectra for 2  $\mu\text{m}$  thick GaN homoepitaxial layer grown by HVPE on bulk GaN substrate (courtesy of Dr. J. Freitas, Jr.). The FWHM of the PL peak is below 0.5 meV.

True bulk technical approach involving boule growth on a native seed has substantial potential for material quality improvement by selecting the best quality seed for each subsequent growth run. However,

many technical issues, including relatively low growth rate and long-term process and equipment instability, have to be resolved before this technique will be commercially valuable.

## 5.2. Device Applications

Multi layer structures grown by HVPE were used for the fabrication of several types of GaN-based devices including electronic and optoelectronic devices, HEMTs<sup>90</sup> and LEDs.<sup>91, 92, 38, 93</sup> For all these devices, the whole device epitaxial structure was grown by HVPE technology.

Transistors were fabricated based on AlGaN/GaN<sup>90, 94</sup> epitaxial structures grown by HVPE. The HEMT structure consisted of a 2  $\mu\text{m}$  thick undoped GaN layer grown on sapphire, followed by a 30 nm thick Al<sub>0.22</sub>Ga<sub>0.78</sub>N layer. Fabricated devices with 1  $\mu\text{m}$  gate length showed transconductances in excess of 110 mS/mm and drain-source current above 0.6 A/mm. A current gain cut-off frequency,  $f_t$ , of 11.5 GHz and a maximum frequency of oscillation,  $f_{\text{max}}$ , of 20.65 GHz were achieved for 1x100  $\mu\text{m}^2$  device at a gate voltage of 0 V and drain voltage of 2 V (Fig. 29).<sup>95</sup>

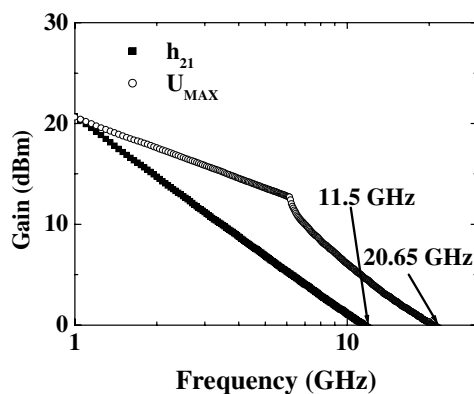


Fig. 29. RF frequency response of a 1x100  $\mu\text{m}^2$  gate dimension HVPE AlGaN/GaN HEMT measured at  $V_g = 0$  V and  $V_{ds} = 3$  V<sup>96</sup>.

Blue,<sup>92</sup> ultra violet (Fig. 30),<sup>38,93</sup> and white LEDs were fabricated based on AlGaN/GaN and AlGaN/AlGaN p-n heterostructures grown by

HVPE. Peak wavelength for HVPE blue LEDs ranged from 415 to 420 nm. Packaged LEDs had output power and external efficiency up to 1.4 mW and 2.5 %, respectively. These numbers represent highest external efficiency reported for In-free LED structures emitting in the blue-violet spectral region. Recently, HVPE grown blue LEDs have been used for sign fabrication.<sup>96</sup>

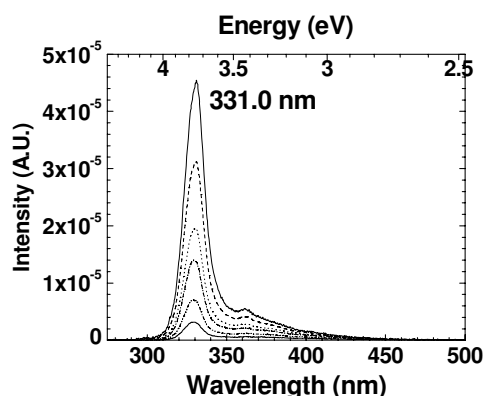


Fig. 30. EL spectra at various currents measured for AlGaIn/AlGaIn double heterostructure UV LED grown on sapphire by HVPE at TDI, Inc. Peak emission is at 331 nm.

AlGaIn/AlGaIn double heterostructures for UV LED were grown by HVPE on sapphire substrates. Peak wavelength for HVPE grown UV LEDs was controlled from 300 to 350 nm by varying AlN content in the light-emitting region. For packaged 340 nm LED (Fig. 28) 2 mW output power was measured at 110 mA pulsed current.<sup>38</sup>

## 6. Conclusions

The technology of group III nitride epitaxy and bulk growth has shown grate progress in the last decade. It appears that HVPE is the current choice of technology for GaN and AlN substrate materials including template, free standing, and bulk substrates. Resent demonstration of 6-inch GaN and AlN HVPE technology and multi wafer growth HVPE equipment are important steps toward large area low cost substrate

materials. However, defect densities are still higher than  $10^5 \text{ cm}^{-2}$  and growth rate itself is below 1 mm/hr required for true bulk crystal growth.

New achievements in the HVPE field include fabrication of HVPE grown multi layer device structures with sharp interfaces, LEDs and HEMTs. The technology progressing very rapidly and we expect dramatic progress to be achieved in a few years in both scientific and industrial aspects of group III nitride HVPE technology.

### Acknowledgments

Authors would like that thank O. Kovalenkov, V. Soukhoveev, Y. Shapovalova, V. Ivantsov, A. Syrkin, V. Maslennikov, Yu. Melnik, A. Nikolaev, A. Cherenkov, and V. Syzov for their priceless input into technological developments described in this paper. Experimental results described in this paper have been achieved in collaboration with a large number of academic, government, and industrial organizations. Authors are very grateful to all colleagues who supported this work. Materials characterizations performed by M. Reshchikov, S. Nikishin, J. Freitas, C. Collins, M. Wraback, M. Kneissl, N. Johnson, N. Shmidt, V. Davidov, A. Davydov, N. Kuznetsov, T. Dang, D. Thomson, and D. Look made these developments possible. We thank Leighton Electronics, Inc Candela, and Accent Optical Technologies for their help in material investigation. Encouraging and governing discussions with C. Wood, M. Yoder, and J. Carrano and their support were very important for this work. Financial support for HVPE development at TDI was provided by the Department of Defense, Department of Energy, and Department of Commerce.

### References

1. H.P. Maruska and J.J. Tietjen, The preparation and properties of vapor-deposited single-crystalline GaN, *Appl. Phys. Lett.* **15**, 10, 327-329 (1969).
2. W.M. Yim, E.J. Stofko, P.J. Zanzucchi, J.I. Pankove, M. Ettenberg, and S.L. Gilbert, Epitaxially grown AlN and its optical band, *J. Appl. Phys.* **44**, 1, 292-296 (1973).
3. J.I. Pankove, E.A. Miller, D. Richman, and J.E. Berkeyheiser, Electroluminescence in GaN, *Journal of Luminescence*, **4**, 63-66 (1971).
4. J. Hagen, R.D. Metcalfe, D. Wickenden, and W. Clark, Growth and properties of  $\text{Ga}_x\text{Al}_{1-x}\text{N}$  compounds, *J. Phys. C: Solid State Phys.* **11**, L143-L146 (1978).

5. H. Amano, M. Kito, K. Hiramatsu and I. Akasaki, P-Type Conduction in Mg-Doped GaN Treated with Low-Energy Electron Beam Irradiation (LEEBI), *Jap. J. Appl. Phys.* **28**, N12, pp. L2112-L2114 (1989).
6. J. S. Nakamura, T. Mukai and M. Senoh, High-Power GaN P-N Junction Blue-Light-Emitting Diodes, *Jap. J. Appl. Phys.* **30**, N12A, pp. L1998-L2001 (1991).
7. S. Nakamura and G. Fasol, *The Blue Laser Diode – GaN-Based Light Emitters and Lasers*, Heidelberg: Springer-Verlag (1997).
8. K. Naniwae, S. Itoh, H. Amano, K. Itoh, K. Hiramatsu, and I. Akasaki, Growth of single crystal GaN substrates using hydride vapor phase epitaxy, *J. Cryst. Growth* **99**, 381-384 (1990).
9. S.T. Kim, Y.J. lee, D.C. Moon, C.H. Hong, T.K. Yoo, Preparation and properties of free-standing HVPE grown GaN substrates, *J. Cryst. Growth* **194**, 37-42 (1998).
10. Yu. Melnik, A. Nikolaev, I. Nikitina, K. Vassilevski, V. Dmitriev, Properties of free-standing GaN bulk crystals grown by HVPE, *Mat. Res. Soc. Symp. Proc. Vol. 482*, 269-274 (1998).
11. D.C. Look, J.R. Sizelove, J. Jasinski, Z. Liliental-Weber, K. Saarinen, S.S. Park, and J.H. Han, Electrical, Optical, Structural, and Analytical Properties of Very Pure GaN, *Mat. Res. Soc. Symp. Proc. Vol. 743*, 575-590 (2003).
12. A. Usui, Bulk GaN crystal with low defect density grown by hydride vapor phase epitaxy, *Mat. Res. Soc. Symp. Proc. Vol. 482*, 233-244 (1998).
13. M. Albrecht, I.P. Nikitina, A.E. Nikolaev, Yu.V. Melnik, V.A. Dmitriev, and H.P. Strunk, Dislocation Reduction in AlN and GaN Bulk Crystals Grown by HVPE, *Phys. Stat. Sol. (a)*, **176**, 453-458 (1999).
14. L. Liu, J.H. Edgar, Substrates for gallium nitride epitaxy, *Material Science and Engineering R* **37**, 61-127 (2002).
15. O. Ambacher, Growth and applications of Group III-nitrides, *J. Phys. D: Appl. Phys.* **31**, 2653-2710 (1998).
16. S.Yu. Karpov, A.S. Segal, D.V. Zimina, S.A. Smirnov, A.P. Sid'ko, A.V. Kondratyev, Y.N. Makarov, D. Martin, V. Wagner, and M. Ilegems, Transport and Chemical Mechanisms in GaN Hydride Vapor Phase Epitaxy, *Mat. Res. Soc. Symp. Proc. Vol. 743* (2003)
17. A. Kazimirov, N. Faleev, H. Temkin, M.J. Bedzyk, V. Dmitriev, Yu. Melnik, High-resolution x-ray study of thin GaN films on SiC, *J. Appl. Phys.* **89**, **11**, 6092-6097 (2001).
18. A.E. Nikolaev, S.V. Rendakova, I.P. Nikitina, K.V. Vassilevski, and V.A. Dmitriev, GaN Grown by Hydride Vapor Phase Epitaxy on p-Type 6H-SiC layers, *J. Electron. Materials* **27**, 288-291 (1998).
19. E. Danielsson, C-M. Zetterling, M. Ostling, A. Nikolaev, I.P. Nikitina, and V. Dmitriev, Fabrication and Characterization of Heterojunction Diodes with HVPE-Grown GaN on 4H-SiC, *IEEE Transactions on Electron Devices*, **48**, 444-449 (2001).

20. A.E. Nikolaev, Yu.V. Melnik, N.I. Kuznetsov, A.M. Strelchuk, A.P. Kovarsky, K.V. Vassilevski, and V.A. Dmitriev, GaN pn-structures grown by hydride vapor phase epitaxy, *Mat. Res. Soc. Symp. Proc.* Vol. **482**, 251-256 (1998).
21. A. Usikov, O. Kovalenkov, V. Ivantsov, V. Soukhoveev, V. Dmitriev, N. Shmidt, D. Poloskin, V. Petrov, V. Ratnikov, P-type GaN epitaxial layers and AlGaIn/GaN heterostructures with high hole concentration and mobility grown by HVPE, *Mater. Res. Soc. Symp. Proc.* Vol. **831**, 453-457 (2005).
22. N.I. Kuznetsov, A.E. Nikolaev, A.S. Zubrilov, Yu.V. Melnik, V.A. Dmitriev, Insulating GaN:Zn layers grown by hydride vapor phase epitaxy on SiC substrates, *Appl. Phys. Lett.* **75**, 3138-3140 (1999).
23. A.Y. Polyakov et al., Studies of deep centers in high-resistivity p-GaN films doped with Zn and grown on SiC by hydride vapor phase epitaxy, *Solid-State Electronics* **45**, 249-253 (2001).
24. I. Akasaki and M. Hashimoto, Infrared lattice vibration of vapour-grown AlN, *Solid State Communications*, **5**, 851-853 (1967).
25. M.P. Callaghan, E. Patterson, B.P. Richards and C.A. Wallace, The growth, crystallographic and electrical assessment of epitaxial layers of aluminum nitride on corundum substrates, *J. Crystal Growth* **22**, 85-98 (1974).
26. T. Yamane, H. Murakami, Y. Kangawa, Y. Kumagai, and A. Koukitu, Growth of thick AlN layer on sapphire (0001) substrate using hydride vapor phase epitaxy, *Phys. Stat. Sol. (c)* **2**, 2062-2065 (2005).
27. A. Nikolaev, I. Nikitina, A. Zubrilov, M. Mynbaeva, Yu. Melnik, V. Dmitriev, AlN wafers fabricated by hydride vapor phase epitaxy, *Mat. Res. Soc. Symp.* **595**, W6.5.1-W6.5.5 (2000).
28. Yu. Melnik, D. Tsvetkov, A. Pechnikov, I. Nikitina, N. Kuznetsov, V. Dmitriev, Characterization of AlN/SiC epitaxial wafers fabricated by hydride vapour phase epitaxy, *Phys. Stat. Sol. (a)* **188**, N1, 463-466 (2001).
29. D. Tsvetkov, Yu. Melnik, A. Davydov, A. Shapiro, O. Kovalenkov, J.B. Lam, J.J. Song, V. Dmitriev, Growth of submicron AlGaIn/GaN/AlGaIn heterostructures by hydride vapor phase epitaxy (HVPE), *Phys. Stat. Sol. (a)* **188**, N1, 429-432 (2001).
30. A.S. Usikov, Dae-Woo Kim, A.I. Pechnikov, Yu.V. Ruban, M.A. Mastro, Yu. Melnik, V.A. Soukhoveev, O.V. Kovalenkov, G.H. Gainer, S. Mahajan, V.A. Dmitriev, Material quality improvements for homoepitaxial GaN and AlN layers grown on sapphire-based templates, *Phys. Stat. Sol. C*, **N7**, 2580-2584 (2003).
31. O. Kovalenkov, V. Soukhoveev, V. Ivantsov, A. Usikov, V. Dmitriev, Thick AlN layers grown by HVPE, *J. Cryst. Growth* **281**, 87-92 (2005).
32. J.R. LaRoche, B. Luo, F. Ren, K.H. Baik, D. Stodilka, B. Gila, C.R. Abernathy, S.J. Pearton, A. Usikov, D. Tsvetkov, V. Soukhoveev, G. Gainer, A. Pechnikov, V. Dmitriev, G.-T. Chen, C.-C. Pan, J.-I. Chyi, GaN/AlGaIn HEMTs grown by hydride vapor phase epitaxy on AlN/SiC substrates, *Solid State Electronics* **48**, 193-196 (2004).

33. B. Baranov, L. Daweritz, V.B. Gutan, G. Jungk, H. Neumann, and H. Raidt, Growth and properties of  $\text{Al}_x\text{Ga}_{1-x}\text{N}$  epitaxial layers, *Phys. Stat. Sol. (a)* **49**, 629-636 (1978).
34. K.H. Kim, J.Y. Yi, H.J. Lee, M. Yang, H.S. Ahn, C.R. Cho, S.W. Kim, S.C. Lee, Y. Honda, M. Yamaguchi, and N. Sawaki, Growth of thick AlGa $\text{N}$  by metalorganic-hydride vapor phase epitaxy, *Phys. Stat. Sol. (c)* **1**, 2474-2477 (2004).
35. N.A. Sanford, L.H. Robins, A.V. Davydov, A. Shapiro, D.V. Tsvetkov, V.A. Dmitriev, S. Keller, U.K. Mishra, and S.P. DenBaars, Reflective index study of  $\text{Al}_x\text{Ga}_{1-x}\text{N}$  films grown on sapphire substrates, *J. Appl. Phys.* **94**, 2980-2991 (2003).
36. G.A. Onushkin, A.E. Nikolaev, A.V. Fomin, O.Yu. Ledyayev, A.E. Cherenkov, E.V. Kalinina, I.P. Nikitina, O.V. Kovalenkov, and V.A. Dmitriev, Photoelectrical Properties of AlGa $\text{N}$  Epitaxial Layers Grown by HVPE, *Phys. Stat. Sol. (c)* **1**, 465-468 (2002).
37. Yu.V. Melnik, A.E. Nikolaev, S.I. Stepanov, A.S. Zubrilov, I.P. Nikitina, K.V. Vassilevski, D.V. Tsvetkov, A.I. Babanin, Yu.G. Musikhin, V.V. Tretyakov and V.A. Dmitriev, AlN/GaN and AlGa $\text{N}$ /GaN heterostructures grown by HVPE on SiC substrates, *Mat. Res. Soc. Symp. Proc. Vol.* **482**, 245-249 (1998).
38. G.A. Smith, T.N. Dang, T.R. Nelson, J.L. Brown, D. Tsvetkov, A. Usikov, V. Dmitriev, 341 nm emission from hydride vapor-phase epitaxy ultraviolet light-emitting diodes, *J. Appl. Phys.* **95**, 8247 (2004).
39. L.A. Marasina, I.G. Pichugin, M. Tlaczala, Preparation of InN epitaxial layers in  $\text{InCl}_3 - \text{NH}_3$  System, *Kristall und Technik*, **12**, **6**, 541 – 545 (1977).
40. H. Sunakawa, A.A. Yamaguchi, A. Kimura and A. Usui, Growth of InN by chloride-transport vapor phase epitaxy, *Jpn. J. Appl. Phys.* **35**, L1395 – L1397 (1996).
41. Y. Sato and S. Sato, *J. Cryst. Growth* **144**, 15 (1994).
42. Y. Kumagai, K. Takemoto, T. Hasegawa, A. Koukitu, H. Seki, Thermodynamics on tri-halide vapor-phase epitaxy of GaN and  $\text{In}_x\text{Ga}_{1-x}\text{N}$  using  $\text{GaCl}_3$  and  $\text{InCl}_3$ , *J. Cryst. Growth* **231**, 57-67 (2001).
43. N. Takahashi, J. Ogasawara, A. Koukitu, Vapor phase epitaxy of InN using InCl and  $\text{InCl}_3$  sources, *J. Cryst. Growth* **172**, 298-302 (1997).
44. N. Takahashi, R. Matsumoto, A. Koukitu and H. Seki, Growth of InN at high temperature by halide vapor phase epitaxy, *Jpn. J. Appl. Phys.* **36**, L743 – L745 (1997).
45. N. Takahashi, R. Matsumoto, A. Koukitu and H. Seki, Vapor Phase Epitaxy of  $\text{In}_x\text{Ga}_{1-x}\text{N}$  using  $\text{InCl}_3$ ,  $\text{GaCl}_3$  and  $\text{NH}_3$  sources, *Jpn. J. Appl. Phys.* **36**, L601 – L603 (1997).
46. Y. Sato and S. Sato, Hydride Vapor Phase Epitaxy of  $\text{In}_x\text{Ga}_{1-x}\text{N}$  Thin Films, *Jpn. J. Appl. Phys.* **36**, 4295-4296 (1997).
47. A. Syrkin, A. Usikov, V. Soukhoveev, O. Kovalenkov, V. Ivantsov, V. Dmitriev, C. Collins, E. Readinger, N. Schmidt, V. Davydov, S. Nikishin, V. Kuryatkov, D. Song, D. Rosenbladt, M. Holtz, InN-based heterostructures grown by modified HVPE,

- Abstracts of the 6th International Conference on Nitride Semiconductors, August 28-September 2, 2005, Bremen, Germany.
48. J. Wu, W. Walukiewicz, *Superlattices and Microstructures* **34**, 63–75(2003).
  49. H.P. Maruska, W.C. Rhines, and D.A. Stevenson, Preparation of Mg-doped GaN diodes exhibiting violet electroluminescence, *Mat. Res. Bull.* Vol. **7**, 777-782 (1972).
  50. M.A. Mastro, D.V. Tsvetkov, A.I. Pechnikov, A. Soukhoveev, G.H. Gainer, A. Usikov, V. Dmitriev, B. Luo, F. Ren, K.H. Baik, S.J. Pearton, AlGaIn/GaN heterostructures grown by HVPE: growth and characterization, *Mat. Res. Soc. Symp. Proc.* Vol. **764**,39-44 (2003).
  51. G. Seryogin, I. Shalish, W.M. Chan, and V. Narayanamurti, Catalytic Growth of GaN Nanowires by Hydride Vapor Phase Epitaxy, Abstracts of the 2004 MRS Fall Meeting, Boston, MA, November 29-December 3, p.148 (2004).
  52. M. Mynbaeva, D. Tsvetkov, *Inst. Phys. Conf. Ser.* **155**, 365-368 (1997).
  53. M. Mynbaeva, A. Titkov, A. Kryganovskii, V. Ratnikov, and K. Mynbaev, Structural characterization and strain relaxation in porous GaN layers, *Appl. Phys. Lett.* **76**, 1113-1115 (2000).
  54. M. Mynbaeva, A. Titkov, A. Kryzhanovski, I. Kotousova, A.S. Zubrilov, V.V. Ratnikov, V.Yu. Davydov, N.I. Kuznetsov, K. Mynbaev, D.V. Tsvetkov, S. Stepanov, A. Cherenkov and V.A. Dmitriev, Strain relaxation in GaN layers grown on porous GaN sublayers, *MRS Internet Journal Nitride Semiconductor Research*, **4**, 14 (1999).
  55. R.L. Aggarwal, P.A. Maki, R.J. Molnar, Z.-L. Liao, and I. Melngailis, Optically pumped GaN/Al<sub>0.1</sub>Ga<sub>0.9</sub>N double-heterostructure ultraviolet laser, *J. Appl. Phys.* **79**, 2148-2150 (1996).
  56. Yu. Melnik, A. Nikolaev, S. Stepanov, I. Kalinina, K. Vassilevski, A. Ankudinov, Yu. Musikhin and V. Dmitriev, HVPE GaN and AlGaIn “Substrates” for Homoepitaxy, *Materials Science Forum* Vols. **264-268**, 1121-1124 (1998).
  57. K.S. Boutros, J.S. Flynn, V. Phanse, R.P. Vaudo, G.M. Smith, and J.M. Redwing, InGaIn double-heterostructures and DH-LEDs on HVPE GaN-on-sapphire substrates, *Mat. Res. Soc. Symp. Proc.* Vol. **482**, 1047-1052 (1998).
  58. V. Dmitriev, A. Nikolaev, A. Cherenkov, D. Tsvetkov, S. Stepanov, N. Kuznetsov, I. Nikitina, A. Kovarsky, M. Yagovkina, V. Davidov, Properties of GaN homoepitaxial layers grown on GaN epitaxial wafers, *Mat. Res. Soc. Symp. Proc.* Vol. **512**, 451-456 (1998).
  59. K. Naniwae, S. Itoh, H. Amano, K. Itoh, K. Hiramatsu and I. Akasaki, Growth of single crystal GaN substrates using hydride vapor phase epitaxy, *J. Cryst. Growth* **99**, 381-384 (1990).
  60. R.J. Molner, W. Gotz, L.T. Romano, N.M. Johnson, Growth of gallium nitride by hydride vapor-phase epitaxy, *J. Cryst. Growth.* **178**, 147-156 (1997).

61. P.A. Maki, R.J. Molner, R.L. Aggarwal, Z-L. Liao, and I. Melngailis, Optically Pumped GaN-AlGa<sub>N</sub> Double-Heterostructure Lasers Grown by ECR-GSMBE and HVPE, *Mat. Res. Soc. Symp. Proc.* Vol. **395**, 919-924 (1996).
62. J.W. Johnson, J. Han, A.G. Baca, R.D. Briggs, R.J. Shul, J.R. Wendt, C. Monier, F. Ren, B. Luo, S.N.G. Chu, D. Tsvetkov, V. Dmitriev, S.J. Pearton, Comparison of AlGa<sub>N</sub>/Ga<sub>N</sub> high electron mobility transistors grown on AlN/SiC templates or sapphire, *Solid-State Electronics* 46 (2002) 513-523.
63. M.J. Manfra, L.N. Pfeiffer, K.W. West, H.L. Stomer, K.W. Baldwin, J.W.P. Hsu, D.V. Lang, R.J. Molnar, High-mobility AlGa<sub>N</sub>/Ga<sub>N</sub> heterostructures grown by molecular-beam epitaxy on Ga<sub>N</sub> templates prepared by hydride vapor phase epitaxy, *Appl. Phys. Lett.* **77**, 2888-2890 (2000).
64. V. Schwegler, C. Kirchner, M. Seyboth, M. Kamp, K.J. Ebeling, Yu.V. Melnik, A.E. Nikolaev, D. Tsvetkov, and V.A. Dmitriev, Ga<sub>N</sub>/SiC Quasi-Substrates for Ga<sub>N</sub>-based LEDs, *Phys. Stat. Sol. (a)* **176**, 99-102 (1999).
65. Y. Shibata, A. Motogaito, H. Miyake, K. Hiramatsu, Y. Ohuchi, H. Okagawa, K. Tadamoto, T. Nomura, Y. Hamamura, and K. Fukui, Fabrication and characterization of UV Schottky detectors by using a freestanding Ga<sub>N</sub> substrates, *Mat. Res. Soc. Symp. Proc.* Vol. 831 (2005) 137-142.
66. M. Kneissl, Z.H. Zang, M. Teepe, C. Knollenberg, N.M. Johnson, S.B. Schujman, L.J. Schowalter, A. Usikov, and V. Dmitriev, reported at the 6th International Conference on Nitride Semiconductors, August 28-September 2, 2005 Bremen, Germany; to be published.
67. C. Sasaoka, H. Sunakawa, A. Kimura, M. Nido, A. Usui, A. Sakai, High-quality InGa<sub>N</sub> MQW on low-dislocation-density Ga<sub>N</sub> substrate grown by hydride vapor-phase epitaxy, *J. Cryst. Growth* **189/190**, 61-66 (1998).
68. J.K. Gillespie, R.C. Fitch, N. Moser, T. Jenkins, J. Sewell, D. Via, A. Crespo, A.M. Dabiran, P.P. Chow, A. Osinsky, M.A. Mastro, D. Tsvetkov, V. Soukhoveev, A. Usikov, V. Dmitriev, B. Luo, S.J. Pearton, F. Ren, Uniformity of dc and rf performance of MBE-grown AlGa<sub>N</sub>/Ga<sub>N</sub> HEMTS on HVPE-grown buffers, *Solid State Electronics* **47**, 1859-1862 (2003).
69. C. Lee, H.Y. Lee, H. Shin, C. Kim, H. Ko, J. Han, H. Kim, and K. Lee, The influence of threading dislocation density on Hall effects in free-standing Ga<sub>N</sub> substrates, *Phys. Stat. Sol. c*, 2, (2005) 2137-2140.
70. M.K. Kelly, R.P. Vaudo, V.M. Phanse, L. Gorgens, O. Ambacher and M. Stutzmann, Large Free-Standing Ga<sub>N</sub> Substrates by Hydride Vapor Phase Epitaxy and Laser-Induced Liftoff *Jpn. J. Appl. Phys.* **38**, pp. L217-219 (1999).
71. F. Yun, M.A. Reshchikov, K. Jones, P. Visconti, H. Morkoc, S.S. Park, K.Y. Lee, Electrical, structural, and optical characterization of free-standing Ga<sub>N</sub> template grown by hydride vapor phase epitaxy, *Solid-Sate Electronics* **44**, 2225-2232 (2000).
72. O. Kryliouk, M. Reed, M. Mastro, T. Anderson, and B. Chai, Ga<sub>N</sub> substrates: Growth and Characterization, *Phys. Stat. Sol. (a)* **176**, 407-410 (1999).

73. K. Motoki, T. Okahisa, N. Matsumoto, M. Matsushima, H. Kimura, H. Kasai, K. Takemoto, K. Uematsu, T. Hirano, M. Nakayama, S. Nakahata, M. Ueno, D. Hara, Y. Kumagai, A. Koukitu and H. Seki, Preparation of Large Freestanding GaN Substrates by Hydride Vapor Phase Epitaxy Using GaAs as a Starting Substrate, *Jpn. J. Appl. Phys.* **40**, L140-L143 (2001).
74. C.R. Miskys, M.K. Kelly, O. Ambacher, G. Martinez-Criado, and M. Stutzmann, GaN homoepitaxy by metalorganic chemical-vapor deposition on free-standing GaN substrates, *Appl. Phys. Lett.* **77**, 1858-1860 (2000).
75. R.P. Vaudo, X. Xu, A. Salant, J. Malcarne and G.R. Brandes, Characteristics of semi-insulating, Fe-doped GaN substrates, *Phys. Stat. Sol. (a)* **200**, No 1, 18 – 21(2003).
76. B. Monemar, H. Larsson, C. Hemmingsson, I.G. Ivanov, D. Godova, Growth of thick GaN layers with hydride vapour phase epitaxy, *J. Cryst. Growth* **281**, 17-31 (2005).
77. R.P. Vaudo, X. Xu, A. Salant, J. Malcarne, and G.R. Branes, Characterization of semi-insulating, Fe-doped GaN substrates, *Phys. Stat. Sol. a*, 1 (2003) 18-21.
78. P.P. Paskov, T. Paskova, P.O. Holtz, B. Monemar, Polarization-dependent spectroscopy of the near-bandgap excitonic emission in free standing GaN, *Mat. Res. Soc. Symp. Proc. Vol. 798* (2004) 601-606.
79. Yu.V. Melnik, V.A. Soukhoveev, K.V. Tsvetkov, and V.A. Dmitriev, First AlGaIn free-standing wafers, *Mat. Res. Soc. Symp. Proc.* **764**, 363-368 (2003).
80. I. Yonenaga, A. Nikolaev, Yu. Melnik, V. Dmitriev, High-temperature hardness of bulk AlN single-crystal AlN, *Jpn. J. Appl. Phys.* **40**, L426-L427 (2001).
81. B. Luo, J.W. Johnson, O. Kryliouk, F. Ren, S.J. Pearton, S.N.G. Chu, A.E. Nikolaev, Yu. V. Melnik, V.A. Dmitriev, T.J. Anderson, High breakdown M-I-M structures on bulk AlN, *Solid-State Electronics* **46**, 573-576 (2002).
82. D.I. Florescu, V.M. Asnin, F.H. Pollak, *Compound Semicond.* **7**, 61 (1998).
83. S. Nakamura, M. Senoh, S. Nagahama, N. Iwasa, T. Yamada, T. Matsushita, H. Kiyoku. Y. Sugimoto, T. Kozaki, H. Umemoto, M. Sano, and K. Ohocho, Continues-wave operation of InGaIn/GaN/AlGaIn-based laser diodes grown on GaN substrates, *Appl. Phys. Lett.* **72**, 2014-2016 (1998).
84. M. Kuramoto, C. Sasaoka, Y. Hisanaga, A. Kimura, A.A. Yamaguchi, H. Sunakawa, N. Kuroda, M. Nido, A. Usui, and M. Mizuta, Continues-Wave Operation of InGaIn Multi-Quantum-Well Laser Diodes Grown on an n-GaN Substrate with a Backside n-Contact, *Phys. Stat. Sol. (a)* **176**, 35 (1999).
85. T. Nishida and N. Kobayashi, Ten-Milliwatt Operation of an AlGaIn-Based Light Emitting Diode Grown on GaN Substrate, *Phys. Stat. Sol. (a)* **188**, 113-116, (2001).
86. Vladimir Dmitriev, Alexander Fomin, Yuri Melnik, Vitaliy Soukhoveev, Vladimir Ivantsov, Gordon Gainer, and Katie Tsvetkov, Properties of Bulk GaN Wafers and Homoepitaxial Layers, reported at the the International Workshop on Bulk Nitride Semiconductors, May 18th through 23rd, 2002, Amazonas, Brazil [unpublished].

87. X. Xu, R.P. Vaudo, J. Flynn, J. Dion, and G.R. Brandes, MOVPE homoepitaxial growth on vicinal GaN(0001) substrates, *Phys. Stat. Sol. (a)* **5**, 727-731 (2005).
88. D. Hanser, L. Liu, E.A. Preble, D. Thomas, M. Williams, Growth and Fabrication of 2-inch Free-Standing GaN Substrates via the Boule Growth Method, *Mat. Res. Soc. Symp. Proc. Vol. 798*, 257 - 262 (2004).
89. Yu. Melnik et al., AlN substrates: fabrication via vapor phase growth and characterization, *Phys. Stat. Sol. (a)* **1**, 22-25 (2003).
90. M.A. Mastro, D. Tsvetkov, V. Soukhoveev, A. Usikov, V. Dmitriev, B. Luo, F. Ren, K.H. Baik, S.J. Pearton, Hydride vapor phase epitaxy-grown AlGaIn/GaN high electron mobility transistors, *Solid State Electronics* **47**, 1075-1079 (2003).
91. J.B. Lam, G.H. Gainer, S. Bidnyk, A. Elgawadi, G.H. Park, J. Krasinski, J.J. Song, D.V. Tsvetkov, V.A. Dmitriev, Comparative study of HVPE- and MOCVD-grown nitride structures for UV lasing applications, *Mat. Res. Soc. Symp. Proc. Vol. 639*, G6.4.1-G6.4.6 (2001).
92. A.S. Usikov, D.V. Tsvetkov, M.A. Mastro, A.I. Pechnikov, V.A. Soukhoveev, Y.V. Shapovalova, O.V. Kovalenkov, G.H. Gainer, S.Yu. Karpov, V.A. Dmitriev, B.O'Meara, S.A. Gurevich, E.M. Arakcheeva, A.L. Zakhgeim, H. Helava, Indium-free violet LEDs grown by HVPE, *Phys. Stat. Sol. N7*, 2265-2269 (2003).
93. A.S. Usikov, Yu.V. Melnik, A.I. Pechnikov, V.A. Soukhoveev, O.V. Kovalenkov, E. Shapovalova, S.Yu. Karpov, V.A. Dmitriev, HVPE-grown AlN-GaN based structures for UV spectral region, in: M.S. Shur and A. Zukauskas (eds.), *UV Solid-State Light Emitters and Detectors*, 15-29. 2004 Kluwer Academic Publishers.
94. B. Luo et al., HVPE-grown AlGaIn/GaN HEMTs, *Mat. Res. Soc. Symp. Proc. 764*, 45-55 (2003).
95. M.A. Mastro, , D. Tsvetkov, V. Soukhoveev, A. Usikov, V. Dmitriev, B. Luo, F. Ren, K.H. Baik, S.J. Pearton., RF performance of HVPE grown AlGaIn/GaN HEMTs, *Solid-State Electronics* **48**, 179-182 (2004).
96. V. Dmitriev, A.Usikov, H.Helava, B. O'Meara: HVPE offers alternative route to AlGaIn-based UV emitters, *Compound Semiconductors*, Dec. 2004.